ACTA TECHNICA JAURINENSIS
Vol. 17, No. 1, pp. 22-35, 2024
10.14513/actatechjaur.00728

Research Article

The development of a stitch-based strain sensor for woven lashing straps

Norman Lesser[1,*], Bernd Sadlowsky[2]

[1]Institute for BFSV, Ulmenliet 20, 21033 Hamburg, Germany Phone: +49 17641911633
[2]HAW Hamburg University of Applied Sciences, Department of process engineering, Ulmenliet 20, 21033 Hamburg, Germany
[*]E-mail: lesser@bfvs.de

Submitted: 13/12/2023 Accepted: 29/01/2024 Published online: 19/02/2024

Abstract: In this paper the development of a stitch-based strain sensor for lashing straps is discussed. A variety of Three different commercial woven narrow fabric straps were embroidered with conductive yarns in two designed patterns to enable belt tension measurement and monitoring. The applications were tested in a cyclic elongation test and a creep elongation procedure to investigate the strain sensitivity and the influences of the narrow fabric's properties, the stitch design, and the conductive yarn properties. It was found that the developed applications provided a good strain sensing ability but lack in cyclic recovery abilities.

Keywords: smart textiles; strain sensor; lashing strap; load security

I. INTRODUCTION

Woven narrow fabric straps are an essential tool for modern road freight transportation. They play a pivotal role in ensuring a proper load security by lashing down cargo or fixating it in the transport carrier vehicle. During road transportation the transport vehicle accelerating, braking, and manoeuvring is conducting dynamic acceleration forces onto the transported freight. If not properly secured those dynamic acceleration forces will move and shift the transported goods inside of the vehicle and will eventually lead to severe transport damages occurring in the freight or even cause fatal road traffic accidents.

A proper securing procedure requires a precise load securing belt tensioning, which amount of required tension must be calculated precisely in regard of the cargos mass, size and shape. Complex loads may require securing with multiple straps with each belt tension individually adjusted and monitored during the whole transport. [1 - 5] In recent years various research and development projects have successfully implemented stitch-based textile resistive strain sensors for a textile substrates strain and elongation measurement. Especially in medicine and healthcare applications as well as in soft robotics or lightweight construction materials, stitched sensor applications with the ability to sense even tiny amounts of substrate elongation have proven to be promising to solve specific technical problems. [6 - 8]

However, research focusing on stitch-based strain sensors for belt tension measurement of woven lashing straps is relatively rare and the particular use of stitch-based strain sensors for load security monitoring have not been widely explored until this point. CNC-embroidery machines allow smart textile developers to freely design and embroider textile circuitry and conductive pathways onto a broad variety of textile substrates in various dimensional shapes and stages of manufacturing. [9, 10] This paper presents a case study about embroidering narrow fabric straps feasible for object securing and fixation with a stitch-based resistive strain sensor. The aim of this study is to investigate if stitch-based strain sensors are a feasible attempt to measure the applied belt tension while fixating an object and to monitor it during a transport time.

II. STITCH-BASED STRAIN SENSORS

Stitching techniques like sewing and embroidery are some of the oldest textile manufacturing processes known. A stitch is generally formed by a needle penetrating a fabric while guiding a yarn thru it. The Yarn loop with itself or with another present yarn on the fabrics reverse side, locking it form-fitting and by friction force. A stitch can generally be classified by the pattern of its loop formation and its geometrical properties like its stitch length, width, and depth. Stich types are commonly categorized by established standards like ISO 4915:1991. [11, 12]

A Stitch made from a single or multiple conductive yarns conducts electrical current thru a textile fabric acting as a textile conducting element in a circuit. Like every conventional conductor, like for example metal wires, the stitched conductive yarn has a specific electrical resistivity in relaxed condition, which changes when deformation occurs. [13, 14]

The change of the stitch's resistivity can be used as a computable electrical signal to calculate its physical elongation and therefore the stitched fabrics elongation itself. With the general deformation behaviour of the textile substrate known, the working strain can be calculated from the measured resistivity change using the sensors gauge factor. [15] The gauge factor is a proportional factor describing resistivities change in comparison to the sensor's elongation. It is commonly used as an indicator for a strain sensors general level of sensitivity. Other important sensor characteristics are its linearity, describing the proportion in resistance change in relation to the change in working strain., as well as the sensors recovery property. A sensors recovery property describes the ability to maintain its sensing quality after multiple cycles of use without permanent resistance drift or occurring damages decreasing its sensitivity. [16-18]

Conductive fibers spun to conductive yarns and being stitched onto fabric in a certain pattern are far from being ideal conductors. So most conventional models depicting the strain resistive behaviour of metal wires or printed metal films are not suitable to describe or predict a stitch-based strain sensors sensing mechanism or general conductive behaviour. [19] The conductivity and resistivity of a single conductive fiber depends on various factors like for example it's length, width, and square geometry as well as the used functionalization method. Spun yarns may contain several thousands of single conductive fibers entangled with one another. A conductive yarn with a certain length can therefore be depicted as a conductive network of an infinitesimal high number of single conductors short circuiting with one another due to their physical entanglement. In generally a yarns resistivity was found to be positively correlated with its length, meaning that a piece of yarns measured resistivity is higher, the longer it is. [20 - 23]

When a certain Pattern is stitched onto a fabric a certain amount of total yarns length is integrated into the substrate, depending on the stitch's properties like its density, width, and depth. Considering the found positive correlation between a piece of yarns length and its resistivity, stitches with a high stitch density, width, and length, like for example a lockstitch in ZigZag-Pattern, tend to have a higher absolute stitch resistivity than straight lockstitches in comparison. The base resistivity of a stitched sensor application per lengths unit on a fabric's surface therefore depends highly on the stitch's pattern and its properties. [16, 24-26]

When multiple conductive yarns are used to form a stitch, looping, or physically contacting one another due to several loops or conductive yarn sections overlapping causes short circuits leading an overall stitched patterns resistivity to drop. A stitch can be described as a conductive network with its overall resistivity depending mostly on the stitched patterns properties and the presence and concentration of the conductive yarn short circuiting overlapping or cross sectioning loops and entanglement points. (**Fig. 1** and **Fig. 2**) When the fabric is stretched its deformation causes the stitch's width, depths as well as the stitch's density to change as well. When the stitch's properties change and the stitch's geometry seen on the fabrics surface as well deforms, overlapping loops of the conductive yarn separate from one another and cross sectioning areas may shift in contact size and location. These causing former yarn to yarn contact induced short circuits to eventually open and the patterns overall resistivity to change. (**Fig. 3**)

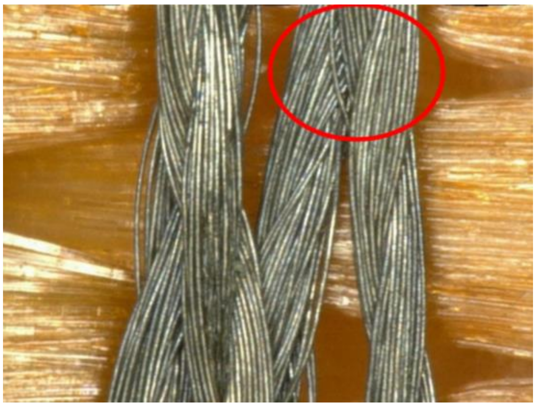

Figure 1. *Overlapping conductive yarn loops*

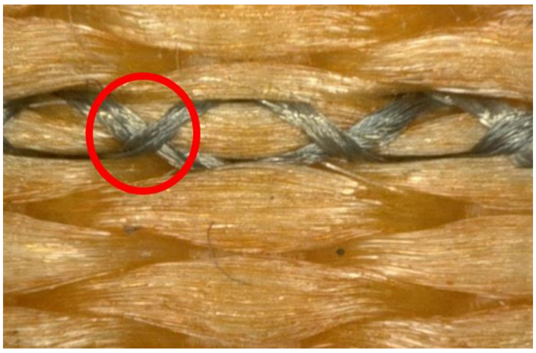

Figure 2*. Cross sectioning conductive yarn loops*

The fabrics and stitch's deformation induces mechanical stress to the conductive yarn. The yarn gets stretched due to the stitch's properties changing. Also, the deformation of the fabric may cause lateral compressive forces to increase locally around the stitch's loop entanglement points. The fabrics deformation will therefore shift the stitch's conductive network as well as the yarns resistive properties itself due to the working mechanical stress.

A stitches overall measured change in resistivity under deformation therefore results both from the combined conductive network changes of yarn and stitched pattern. [27, 28] The fabrics general deformation properties affecting the degree to which its strain induced elongation is conducted to an applied stitch. In reverse the stitch-based application of a yarn onto a fabric and its physical entanglement with it may also affect the fabrics deformation behaviour to some degree. This interaction between the stitch's mechanical deformation characteristics and the fabrics mechanical properties have been the focus of research in the past. A strain sensors functional aspects like its sensitivity, linearity and especially its recovery properties (like its hysteresis error and baseline resistivity drift) have been found to be largely dependent on the stitch's deformation behaviour matching the fabric's. [29] A stitch-based sensors strain sensing behaviour can therefore be described as depending on three main aspects. That being the used conductive yarns resistance changing behaviour under applied strain, the stitch's mechanism of its conductive networking shifting when a fabrics deformation is conducted and at last the stitches and the fabrics deformation behaviour under applied strain interacting with one another.

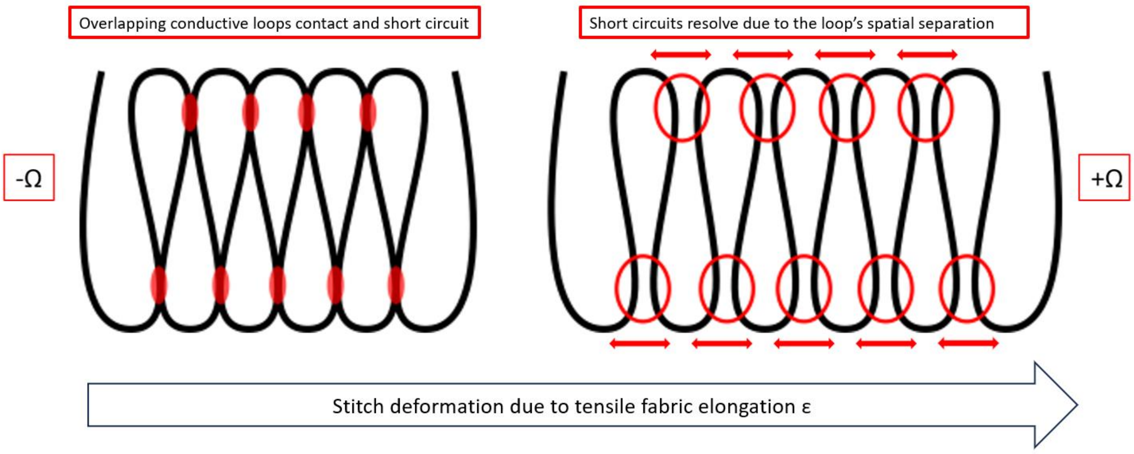

Figure 3. *Schematic representation of the mechanism of increasing resistance by dissolving the yarn contacting*

III. PROBE PREPARATION

Three commercial narrow fabric straps differing in their belt thickness, width, and weight as well as in their maximum tensile strength and stiffness were chosen to be functionalized with a stitch-based strain sensor. All narrow fabric were bought from *Rolf Schwarzbach – Fachhandel (Wipperfürth, GER)* All straps were plain woven from synthetic filament yarns. (**Fig. 4-6**) (**Table 1-2**) In this paper the different narrow fabrics are coded by their product number, given by the supplier. The narrow fabrics were embroidered with two versions of a 304-ZigZag lockstitch using a *ZSK JCZA* computer-controlled embroidery machine *(ZSK Stickmaschinen GmbH, Krefeld (GER))*. Both applications dimensions are illustrated in **Fig. 7**.

Table 1. *Narrow fabric properties*

Narrow fabric	***Fiber material***	***Width [mm]***	***Thickness [mm]***
2.23.100.0105	100% PP	40	1
2.23.200.1600	100% PES	45	1.5
2.23.100.0115	100% PP	50	2.3

Table 2. *Narrow fabric mechanical deformation properties*

Narrow fabric	***Maximum tensile strength F_N [daN]***	***Elongation at maximum tensile strength ε [%]***
2.23.100.0105	404	28.4
2.23.200.1600	1140	23.4
2.23.100.0115	1100	31.2

Both versions varied in their stitch properties to examine their influence on the strain sensing behaviour in comparison. (**Table 3**)

The stitch *ZigZag_V2_Axial* (**Fig. 8-9**) was designed with a particular high stitch density and width. Therefore, a generally high absolute length of conductive yarn was used for this stitch. The second stitch *ZigZag_Double_V2* (**Fig. 10-11**) was composed of two 304-ZigZag lockstitches cross sectioning one another. All probes were embroidered with loose ends for contacting to a multimeter. The individual Probe's consistency is attached in the Appendix (**Table 5**)

Table 3. *Stitch properties*

Stitch Version	***Stitch density***	***Stitch width***	***Stitch depth***
ZigZag_V2_Axial	11 Stitches /10mm	5mm	0.9mm
ZigZag_Double_V2	8 Stitches /10mm	0.8mm	1.2mm

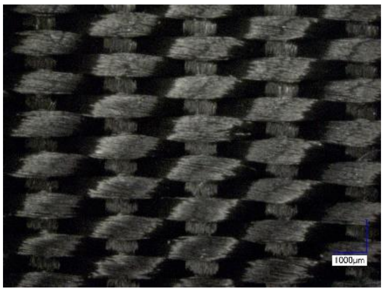

Figure 4 *Narrow fabric surface image 22.23.100.0105"*

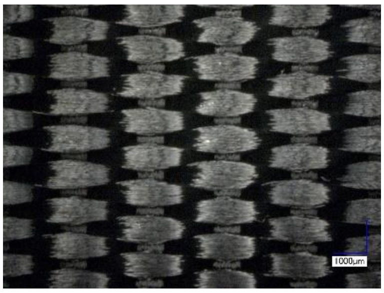

Figure 5. *Narrow fabric surface image 2.23.200.1600"*

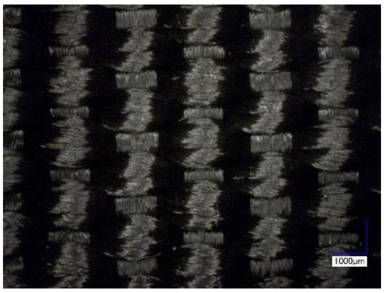

Figure 6. *Narrow fabric surface image 22.23.100.0115"*

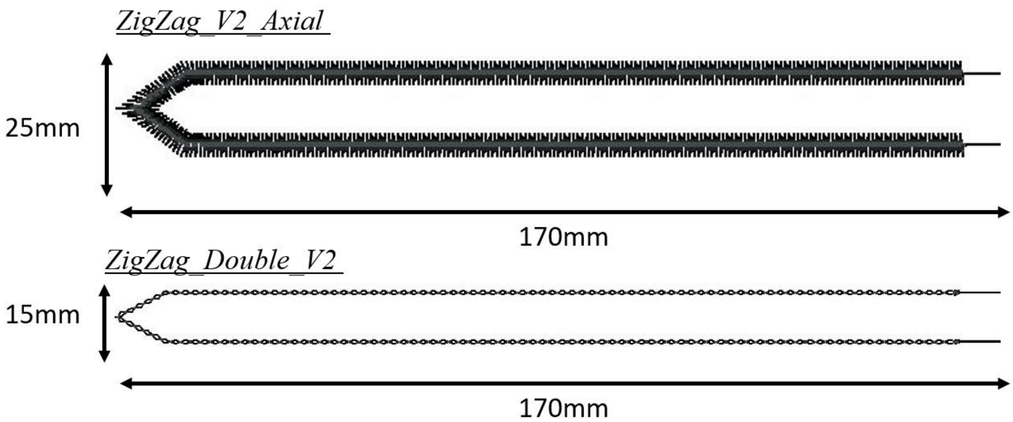

Figure 7. *Stitch dimensions*

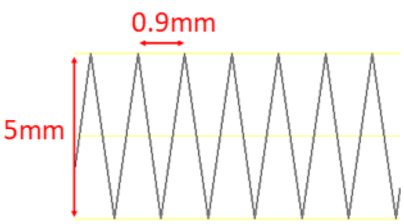

Figure 8. *Stitch properties ZigZag_V2_Axial*

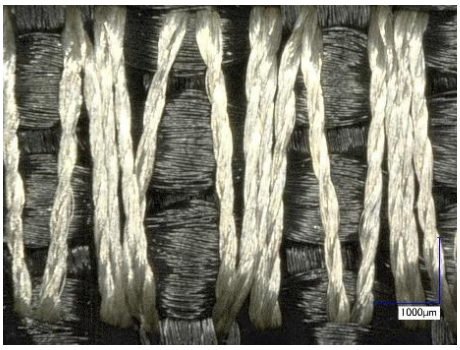

Figure 9. *Microscope image ZigZag_V2_Axial*

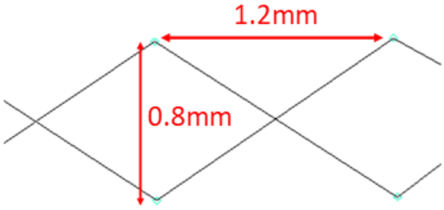

Figure 10. *Stitch properties ZigZag_Double_V2*

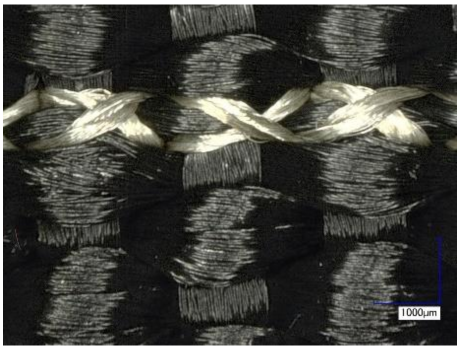

Figure 11. *Microscope Image ZigZag_Double_V2*

The chosen silver-plated yarns *Amann Silver-tech+100* and *Amann Silver-tech+150* (Amann&Söhne GmbH & Co.KG, Bönningheim (GER)) came with a different titer and electrical resistivity per meter yarn length. For the stitch version called *ZigZag_V2_Axial* the non-conductive yarn *Amann ISA Tex 80* was used as a lower yarn. For *ZigZag_Double_V2* the conductive yarns were used as both upper and lower yarns. (**Table 4**)

Table 4. *Yarn properties*

Yarn	***Fiber material***	***Titer [dtex]***	***Yarn resistivity [Ω/m]***
SIlver-Tech+100	100% PA	330	<200
SIlver-Tech+150	100% PA	220	<300
ISA 150	100% PES	180	-

IV. Testing method

The manufactured probes were tensile tested using a *Zwick 1455 20kN (ZwickRoell GmbH & Co. KG, Ulm (GER))* tensile testing machine (**Fig. 12**) with an attached *Elabo R-Meter /SRM 05 (ELABO GmbH, Crailsheim (GER))* multimeter (**Fig. 13**). For tensile testing *Zwick Pneum. Probenhalter Typ 8487 – Fmax.20kN* specimen clamps were installed in the tensile testing machine. For pneumatic probe fixation air pressure of 4 bar was used. The clamps were equipped with ribbed clamping jaws for a better grip in probe fixation. The tensile testing machine was controlled with the testing software TestXpert3 (*ZwickRoell GmbH & Co. KG, Ulm (GER)*). The software allowed the simultaneous measurement of the probe deformation data as well as their electrical resistivity change. The stitches electrical resistivity was measured by connecting the used multimeter to the stitched loose ends using crocodile clamps. (**Fig. 14**)

Figure 12. *Zwick 1455 20kN tensile testing machine*

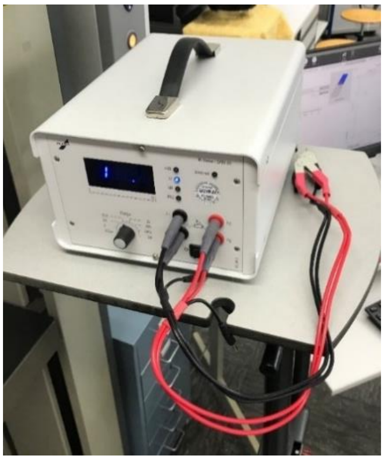

Figure 13. *Elabo R-Meter/SRM 05*

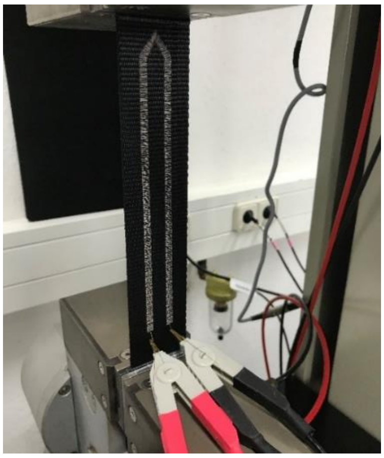

Figure 14. *Loose stitch ends contacted with crocodile clamps*

To investigate the probes strain sensing behaviour two tensile testing procedures were set up in orientation to DIN EN ISO 13934-1. For each test three probes of each combination type were manufactured and tested.

The first testing procedure consisted of the probes controlled cyclic elongation from ε=0% to ε=7%. (**Fig. 15**) The aim of this procedure was to simulate multiple object fixation and release procedures. A maximum elongation of ε=7% was chosen in orientation to DIN EN 12195-2. The probes change in electrical resistivity was plotted alongside the elongation. During this procedure the different probes strain sensitivity and linearity was determined by calculating the probes gauge factor K, using the following formulas (1 – 3).

$$K = \frac{\frac{\Delta R}{R0}}{\frac{\Delta l}{l}} \tag{1}$$

$$\frac{\Delta R}{R0} = k \cdot \frac{\Delta l}{l} = k \cdot \varepsilon \tag{2}$$

$$\varepsilon = \frac{\Delta l}{l} = \frac{\frac{\Delta R}{R0}}{k} \tag{3}$$

where K = gauge factor; R0 = Resistivity [Ω]; l = length [mm]; ε = elongation [%] .

For each deformation cycle the probes strain gauge factors were calculated in intervals of 0.5% elongation. All interval related gauge factors from one cycle were averaged arithmetically and compared in relation to the number of cycles to examine the cyclic wear on the strain sensors. The probes single cycles average gauge factors were then again averaged to compare the different probes sensitivity in general. The sensing linearity was examined by calculating the gauge factors standard deviation for each cycle. A high standard deviation was interpreted as the gauge factor changing volatile in relation to the applied rate of strain. Therefore, a high gauge factor standard deviation was seen as an indicator for a low linearity. The cycles standard deviations were arithmetically averaged to compare the single probes. The second procedure was a creep elongation test where the probes were stretched to an amount of 2000N Force. The probes were locked in their state of elongation after reaching 2000N over 5 Minutes. (**Fig. 16**) This procedure was designed to simulate an object fixation procedure and fixation over a certain amount of transportation time. The harvested data was used to examine if the built belt tension would lose over time due to the fabrics relaxation and if this loosening could be monitored by measuring the stitches resistivity change. The probes absolute resistivity change was plotted alongside the machines applied strain tension Force and the procedures time. Every procedure was tested with stitched probes as well as with unstitched narrow fabric probes and the single conductive yarns for reference. Every narrow fabric probe was cut to a length of 250mm for testing. The single yarn probes were cut to a length of 350mm. Before the testing all probes were exposed to climatization 20°C/65% rel. humidity for 24 hours. All tests were done in a climatized environment with 20°C/65% rel. humidity. The probes narrow fabric length as well as the stitched applications length were measured before every procedure. After the test procedures the tested probes were then again exposed to climatization 20°C/65% rel. humidity for 24 hours and the lengths were again measured for comparison. The stitches resistivity in relaxed state were also measured before and after the testing procedures together with the probe’s length. For length measurements a steel ruler was used. For measuring the probes initial resistivity, a DMM6500 6 ½ multimeter *(Keithley Instruments Inc., Cleveland (USA))* was used

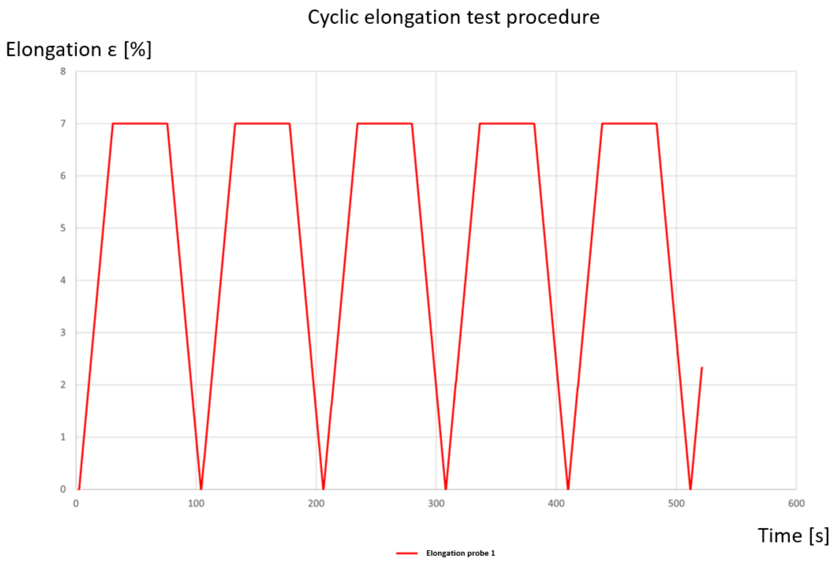

Figure 15. *Cyclic elongation test routine*

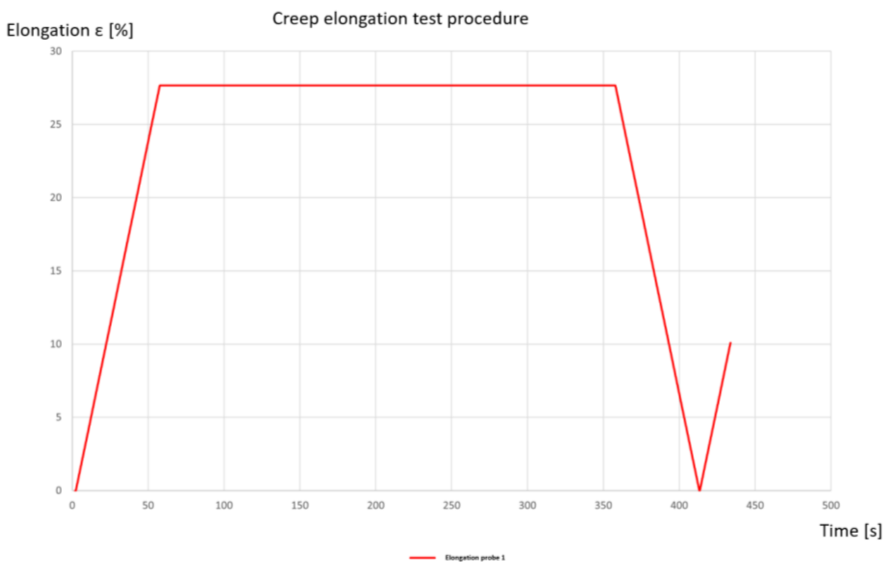

Figure 16. *Creep elongation test routine*

V. Results and Discussion

In this section the experiments result will be presented. The probes strain sensitivity and linearity differ in relation to the composition of narrow fabric, conductive yarn, and stitch type. In **Fig. 17** the probes averaged sensitivity (green) and linearity (blue) is shown. The single probes overall calculated sensitivity is the result of the three composition parameters behaviour under applied strain, interacting with one another.

Probes based on the stitch type ZigZag_Double_V2 tend to provide a higher averaged strain sensitivity than the ZigZag_V2_Axial equivalents. The ZigZag_Double_V2 tend to show a higher sensitivity when Amann Silver-tech+100 is used as conductive yarn. The probes based on ZigZag_V2_Axial show none such tendency. The ZigZag_Double_V2 probes linearity increase when Amann Silver-tech+150 is used, while Amann Silver-tech+150 tends to show a higher linearity with ZigZag_V2_Axial. The probes linearity seems to be mainly dependent on the used yarn, while the sensitivity is particularly influenced by the stitched pattern. The exercised cyclic elongation causes a drift in the sensor applications resistivity and sensitivity, increasing over the number of cycles. The probes measured resistivity at ε=0% to ε=7% elongation increases successively while the working amount of strain Force oppositely decreases. (**Fig. 18-19**) This behaviour can be explained with by the cyclic tensile stress causing wear to the probes. The unstitched reference narrow fabric probes show the same cyclic decrease of loaded tensile force at ε=7% elongation. The comparison of the single probes measured narrow fabrics length and stitch length showed a permanent elongation of both after the experiment. The resistivity drift at ε=0% to ε=7% therefore is likely to be caused by the strain induced permanent deformation, where short circuiting overlapping conductive yarn loops become physically separated from one another and the stitches conductive network permanently alters with every passing elongation cycle. The level of the resistivity increasing and tensile force decreasing at ε=7% elongation alters with individual probe composition. The ZigZag_Double_V2 based probes tend to show a higher resistivity drift caused by cyclic wear then the equivalents based on ZigZag_V2_Axial in comparison. The decreasing amount of the applied tensile force is lower on the probes based on ZigZag_Double_V2 in comparison with ZigZag_V2_Axial. The two stitches different properties therefore influence the probes tensile stiffness. Probes stitched with Amann Silver-tech+150 tend to show a higher relative resistivity drift compared with Amann-Silver-tech+100. The reference tests executed on the single conductive yarns also show that Amann Silver-tech+150 resistivity increases more significantly than Amann Silver-tech+100. The probes resistivity drifting behaviour can therefore be described as mainly caused by the chosen conductive yarn behaviour and the stitches properties as well as by their influence on the fabric tensile stiffness. (**Fig. 20**)

The **Fig. 21** illustrates the probes cyclic strain sensitivity drift for each cycles averaged gauge factor. The red and yellow line illustrate the spread between the first cycle and all cycles gauge factor averaged. The probes based on ZigZag_V2_Axial show a higher resistivity drift with Amann Silver-tech+150, as the increasing spread between the first cycles averaged gauge factor and all cycles averaged gauge factors indicates. With ZigZag_Double_V2 this is the opposite with Amann Silver-tech+100 showing a higher spread. Both illustrations show that the probes individual sensitivity drifting behaviour is highly dependent on the chosen yarn and the narrow fabrics individual cyclic wear behaviour. The probes based on ZigZag_Double_V2 overall show a higher level of cyclic sensitivity drift then ZigZag_V2_Axial. The ZigZag_Double_V2 based probes level of sensitivity drift is closer to the individual conductive yarns calculated drifting behaviour.

Due to the stitch ZigZag_Double_V2 reduced stitch width and increased stitch length, the single stitched loops are aligned in steeper angle to the direction of the working tensile force during probe elongation. The higher loops orientation in the tensile force direction is likely to result in a higher direct tensile stress and stretch working on the yarn in comparison to ZigZag_V2_Axial. (**Fig. 22**) The increased tensile stress causes the yarns conductive network to alter and therefore the resistivity and sensitivity to permanently drift. The stitches sensitivity drifting behaviour approaching the single yarns behaviour at a higher loop orientation indicates that the sensitivity drift of a stitch under cyclic elongation is mainly dependent on the used conductive yarns behaviour and the stitched loops orientation to the direction of force.

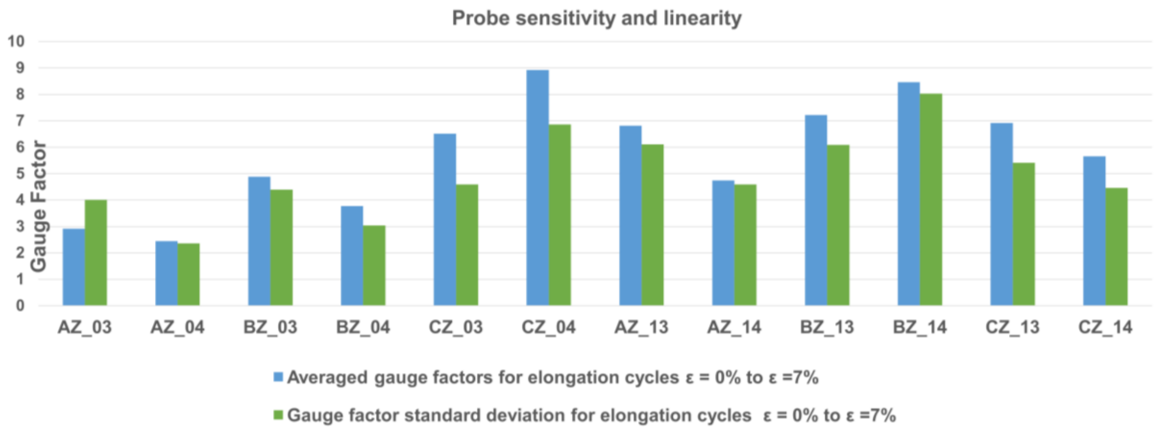

Figure 17*. Probe averaged gauge factors (blue) and gauge factor linear deviation (green)*

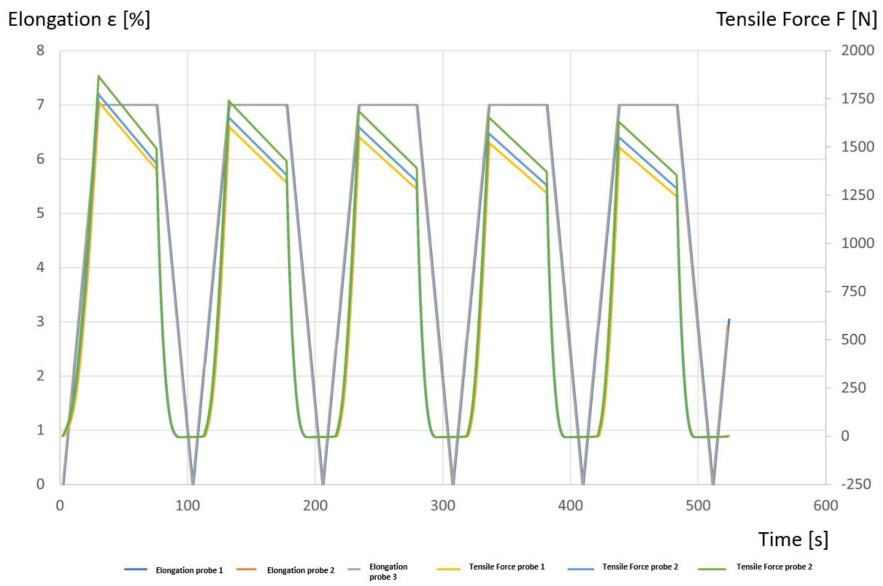

Figure 18*. Probe C_Z0_3 strain force drifting over multiple elongation cycles*

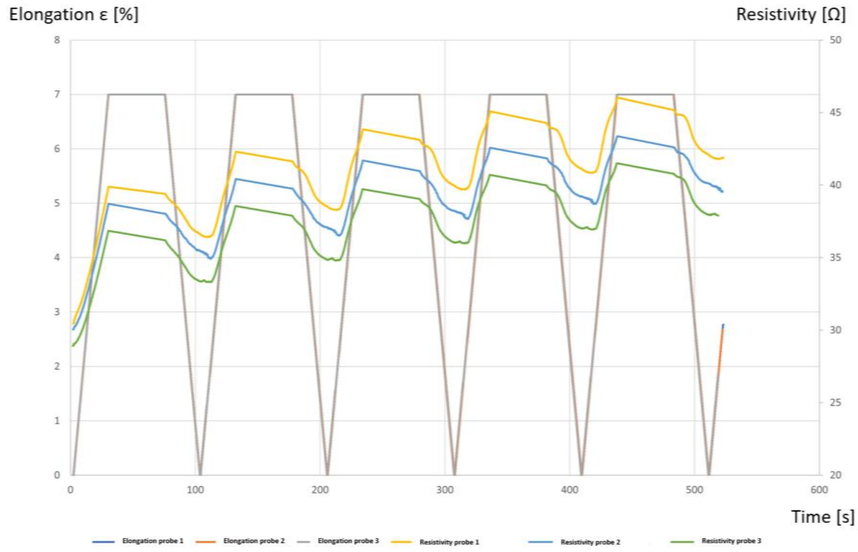

Figure 19. *Probe C_Z0_3 resistivity drift over multiple cycles*

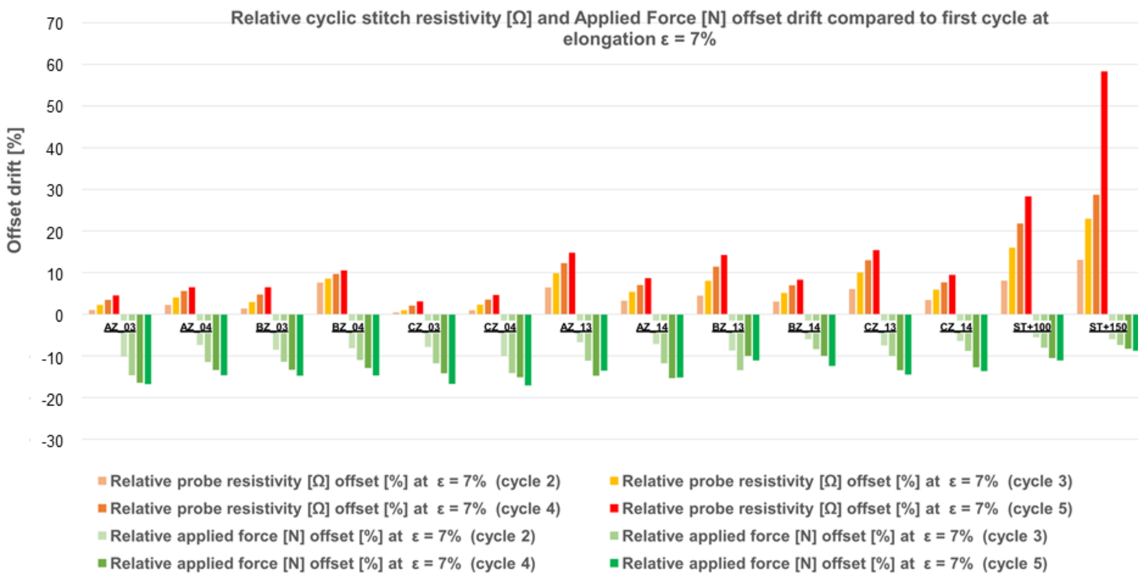

Figure 20. *Probe relative cyclic resistivity drift and relative strain force drift*

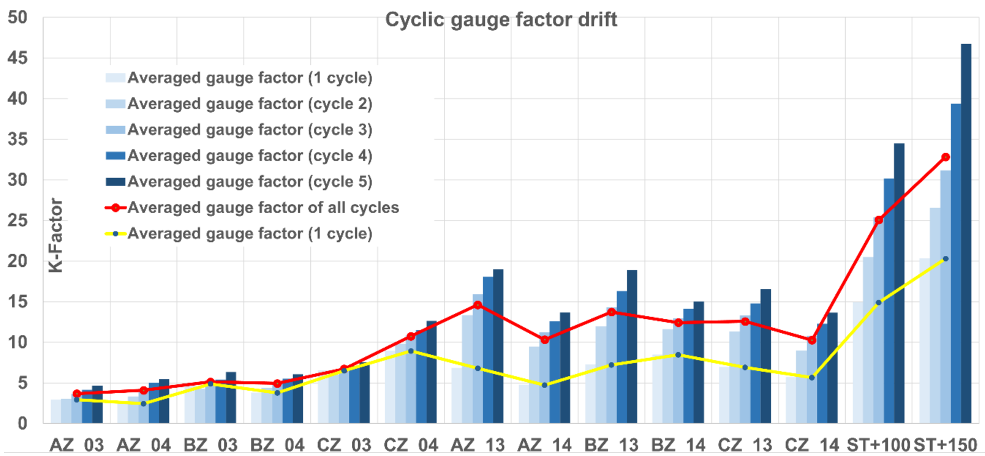

Figure 21. *Probe cyclic strain gauge factor drift*

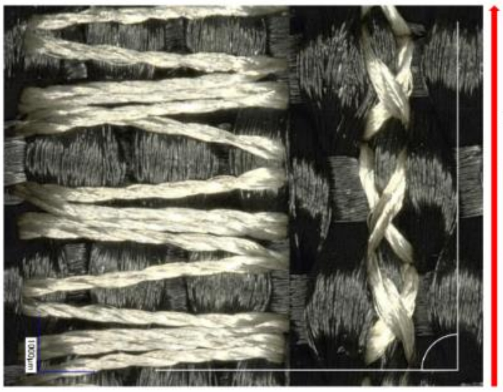

Figure 22. *ZigZag_V2_Axial (left) and ZigZag_Double_V2 (right) loop orientation in applied force direction.*

The conducted creep tests show a regressive decrease of the tensile force working on the stitched and unstitched narrow fabric probes over 275 seconds after first reaching 2000N. This belt tension loosening is expected to be caused by the fabrics woven surface rearranging and the narrow fabrics creep-elongating overtime to reduce the amount of tensile tension. Those fabrics relaxation mechanisms cause the stitches resistivity to alter. In the **Fig. 23** and **24**, the probes decrease in working tensile force and resistivity is exemplary plotted. The fabrics relaxation is conducted to the stitch, causing its conductive network to shift also back into a more relaxed state. To compare the single probes behaviour the stitches range of absolute resistivity change [Ω] is plotted and compared to the relative range of working force [%] decreasing over the creep test time of 275 seconds. (**Fig. 25**) The relative range of working force is interpreted to be mostly dependent on the narrow fabric's physical properties and relaxation behaviour. Though no correlation between the relative range of working force and electrical resistivity is clearly identifiable, the stitched probes resistivity creep alters with the narrow fabric and the yarn. The creep behaviour of ZigZag_V2_Axial is more volatile and likely to be dependent more on the specific narrow fabrics mechanical creep characteristics than ZigZag-Double_V2. ZigZag_V2_Axial behaviour can be explained due to the stitch properties. The fabric surface loosening led to formerly physically separated overlapping loops to reconnect, so the formerly increased stitch resistivity drops back. With the ZigZag_Double_V2 probes this is not the case. The investigation of the occurred permanent elongation and base resistivity drift of all probes shows that the permanent elongation of the fabrics and stitches is higher due to cyclic elongation than to a single long-term exposure to working strain. (**Fig. 26**) The amount of resistivity drift is therefore most likely dependent to the fabrics and stitches grade of permanent elongation. ZigZag_Double_V2 showed a higher resistivity drift which can be explained due to the yarn being damaged because of the sharp angle to the force direction. The amount of elongation is dependent on the fabric's mechanical deformation properties and the recovery ability. So, the occurring drift and therefore wear recovery abilities of the stitched sensors depend highly on the narrow fabric itself.

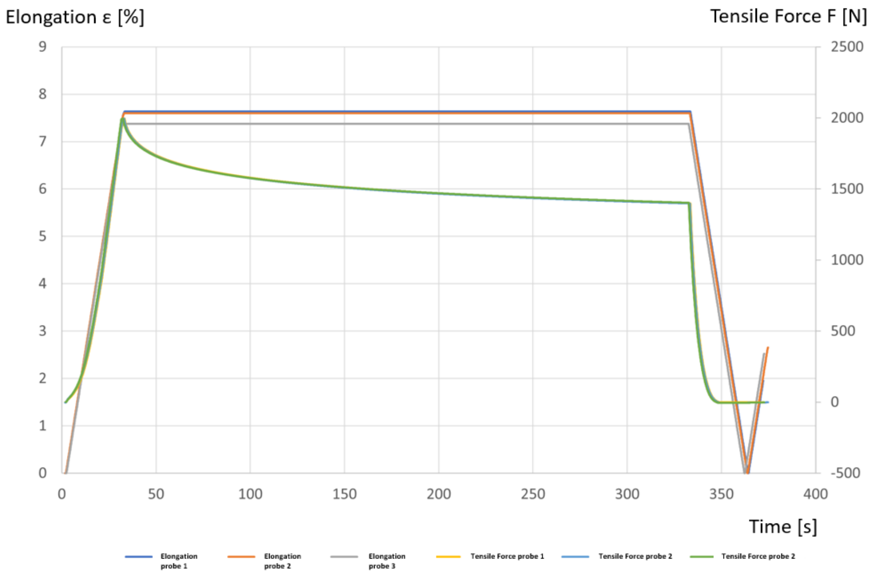

Figure 23. *Probe C_Z0_3 regressive strain force creep*

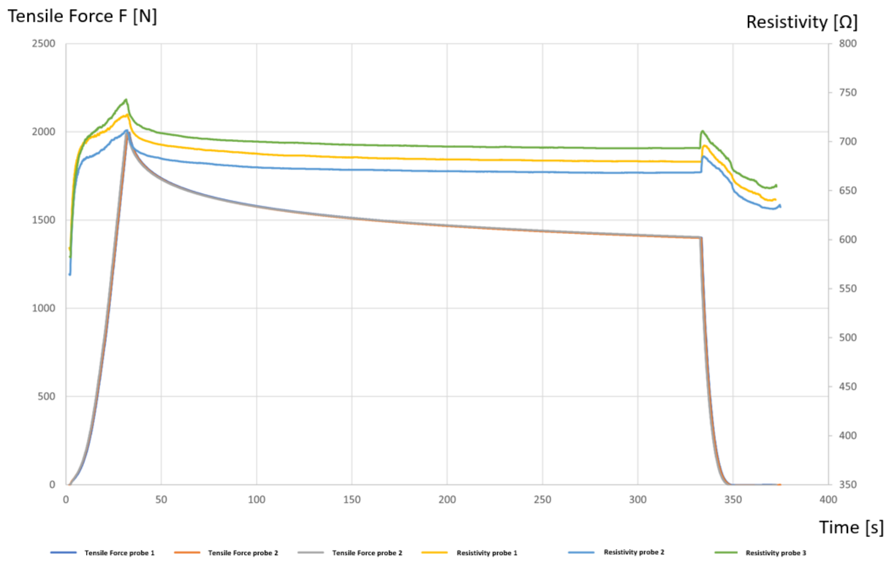

Figure 24. *Probe C_Z0_3 resistivity creep compared with strain force creep*

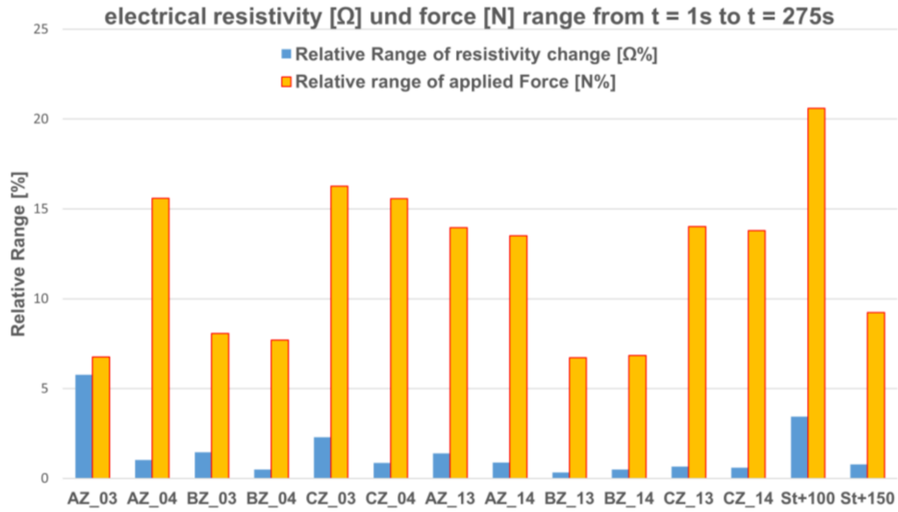

Figure 25. *Probe resistivity and strain force creep behaviour*

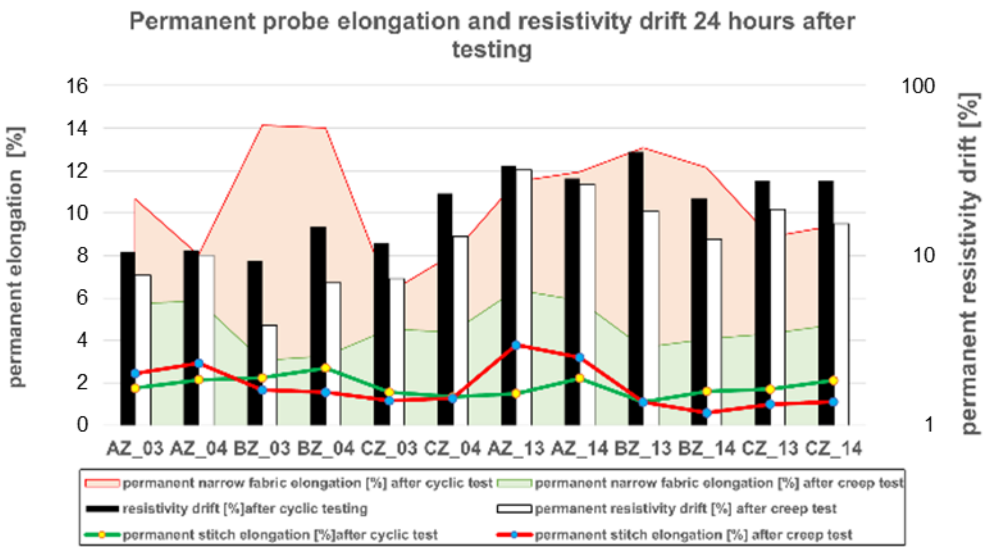

Figure 26. *Probe permanent elongation and resistivity creep 24 hours after testing procedure*

VI. CONCLUSION

The variety of stitch-based sensor applications investigated and examined in this work enabled the elongation measurement and tension monitoring on every chosen narrow fabric strap by measurable resistivity change. The individual probes level of strain sensitivity and linearity heavily depend on the combination of the conductive yarn, the stitch pattern and properties, and the narrow fabrics mechanical deformation characteristics themselves. For this work the strain sensing performance can be therefore described as the result of those three probe parameters interacting during probe deformation. Especially the stitch properties caused yarn loop orientation in tensile force direction highly influences the probes strain sensitivity and linearity. The probes gauge factor increases with a higher orientation, while the linearity decreases. This behaviour is likely to be caused from a higher exposure of the stitched yarn to mechanical stress. All probes show weak recovery properties with resistivity and sensitivity drifts occurring after multiple elongation cycles. This is likely to be caused mainly by the narrow fabrics themselves permanently elongating successively due to cyclic tensile wear, altering the applied stitches conductive network. A higher loop orientation in tensile force direction increases the drifting behaviour and reduces the probes sensor recoverability. The conducted creep elongation experiment's results shows that the narrow fabrics belt tension loosening is monitorable by the sensor applications resistivity altering with the substrates relaxation. The stitches resistivity and the working strain force decrease overtime in a similar regressive plotted curve progression. Although no correlation or regression pattern emerges from the gathered data, the feasibility to monitor the fabrics belt tension depends on the applied stitches properties. The stitch properties influencing the yarns geometrical orientation on the fabric's surface are especially found to significantly influencing the probes strain sensitivity and linearity during the chosen narrow fabric straps tensioning and monitoring. Modern computer-based embroidery provides developers with a broad freedom of stitch pattern design. With further investigation on the single stitch parameters, like stitch width, -length and -density, the use centred development of a stitch-based strain sensor could be a promising attempt for securing belt strain sensing functionalization in the future.

ACKNOWLEDGEMENT

The publishing of this paper was supported by the BFSV institute of Packaging Hamburg

AUTHOR CONTRIBUTIONS

N. Lesser: Conceptualization, Experiments, Theoretical analysis, Writing.

B. Sadlowsky: Supervision and editing.

DISCLOSURE STATEMENT

The authors declare that they have no known competing financial interests or personal relationships that could have appeared to influence the work reported in this paper.

APPENDIX

Table 5. *Manufactured probe combinations*

Probe Name	*Stitch*	*Yarn*	*Narrow fabric*	*Number of tested Probes*
A_Z0_3	ZigZag_V2_Axial	Amann Silver-tech+100	2.23.100.0105	3
A_Z0_4	ZigZag_V2_Axial	Amann Silver-tech+150	2.23.100.0105	3
B_Z0_3	ZigZag_V2_Axial	Amann Silver-tech+100	2.23.200.1600	3
B_Z0_4	ZigZag_V2_Axial	Amann Silver-tech+150	2.23.200.1600	3
C_Z0_3	ZigZag_V2_Axial	Amann Silver-tech+100	2.23.100.0115	3
C_Z0_4	ZigZag_V2_Axial	Amann Silver-tech+150	2.23.100.0115	3
A_Z0_3	ZigZag_Double_V2	Amann Silver-tech+100	2.23.100.0105	3
A_Z0_4	ZigZag_Double_V2	Amann Silver-tech+150	2.23.100.0105	3
B_Z0_3	ZigZag_Double_V2	Amann Silver-tech+100	2.23.200.1600	3
B_Z0_4	ZigZag_Double_V2	Amann Silver-tech+150	2.23.200.1600	3
C_Z0_3	ZigZag_Double_V2	Amann Silver-tech+100	2.23.100.0115	3
C_Z0_4	ZigZag_Double_V2	Amann Silver-tech+150	2.23.100.0115	3

*In each of both testing procedures 3 probes were tested

References

[1] Ladungssicherung auf Straßenfahrzeugen, VDI 2700, (2004), in German

[2] Ladungssicherung auf Straßenfahrzeugen – Berechnung von Sicherungskräften Grundlagen, VDI 2700 Blatt 2 / Part 2, (2014), in German

[3] Ladungssicherung auf Straßenfahrzeugen – Gebrauchsanleitung für Zurrmittel, VDI 2700 Blatt 3.1 / Part 3.1, (2023), in German

[4] Ladungssicherungseinrichtungen auf Straßenfahrzeugen – Sicherheit - Teil 1: Berechnung von Sicherheitskräften, DIN 12195-1, (2021), in German

[5] Ladungssicherungseinrichtungen auf Straßenfahrzeugen – Sicherheit - Teil 2: Zurrgurte aus Chemiefasern, DIN 12195-2, Berlin, (2000), in German

[6] A. Moniruddoza, J. Mersch, P. Schegner, M. Hossain, A. Nocke, C. Chokri, Textilbasierte Sensor-Aktor-Netzwerke für hochpräzise In-Situ-Mechanismen in Faserkunststoffen, Institut für Textilmaschinen und Textile Hochleistungswerkstofftechnik, In: Institut für Textilmaschinen und Textile Hochleistungswerkstoffe, Jahresbericht 2021, Dresden, (2021), pp.1 - 2 in German

[7] R. Nolden, K. Zöll, A. Schwarz-Pfeiffer, Smart Glove with an Arduino-Controlled Textile Bending Sensor, Textile Data Conductors and Feedback Using LED-FSDs™ and Embroidery Technology, Proceedings, 68 (1) (2021) 4. https://doi.org/10.3390/proceedings2021068004

[8] M. Hoerr, E-Textiles – Integration von Elektronik in Textilien durch Stickerei, TEXTILplus (03/04) (2021), pp. 18 – 22, in German

[9] V. Mecnika, M. Hoerr, I. Krievins, S. Jockenhoevel, T. Gries, Technical Embroidery for Smart Textiles: Review, Materials Science. Textile and Clothing Technology, 9 (2014), pp. 56 – 63. https://doi.org/10.7250/mstct.2014.009

[10] G. Golovic, Sewing stitches and seams, In: R. Nayak, Rajkishore, R. Padhye, Woodhead Publishing Series in textiles: Number 168 - Garment Manufacturing Technology, Woodhead Publishing Limited, Cambridge, (2015) p. 247.

[11] Stitches and seams. Classification and terminology of stitch types, ISO 4915:1991, (1991)

[12] B. Moradi, R. Fernández-Garcia, I. Gil, E-Textile Embroidered Metamaterial Transmission Line for Signal Propagation Control, Materials, 11 (6) (2018) 955. https://doi.org/10.3390/ma11060955

[13] J. Eichhoff, A. Hehl, T. Gries, Textile fabrication technologies for embedding electronic functions into fibres, yarns and fabrics, in: T. Kirstein, Woodhead Publishing Series in textiles: Number 139 – Multidisciplinary knowhow for smart-textiles developers Woodhead Publishing Limited, Cambridge, (2013) pp.193 – 223.

[14] K. Jansen, Performance Evaluation of Knitted and Stitched Textile Strain Sensors, Sensors, 20 (24) (2020) 7236. https://doi.org/10.3390/s20247236

[15] P. Regtien, E. Dertien, Sensors for Mechatronics – Second Edition, Elsevier B.V., Amsterdam, (2018) p. 394.

[16] O. Tangsirinaruenart, G. Stylios, A Novel Textile Stitch-Based Strain Sensor for Wearable End Users, Materials, 12 (9) (2019) 1469. https://doi.org/10.3390/ma12091469

[17] S. Keil, Dehnungsmessstreifen - 2. Auflage, Springer Vieweg, Wiesbaden, (2017), p. 485, in German

[18] A. Schwarz, L. Van Langenhove, Types and processing of electro conductive and semiconducting materials for smart textiles, In: T. Kirstein, Woodhead Publishing Series in textiles: Number 139 – Multidisciplinary knowhow for smart-textiles developers Woodhead Publishing Limited, Cambridge, (2013) pp. 28 – 57.

[19] L. Xiuhong, S. Chen, Y. Peng, Z. Zheng, J. Li, F. Zhong, Materials, Preparation Strategies, and Wearable Sensor Applications of conductive Fibers: A Review, Sensors, 22 (8) (2022) 3028. https://doi.org/10.3390/s22083028

[20] J. Xie, M. Miao, Y. Jia, Mechanism of electrical conductivity in metallic fiber-based yarns, AUTEX Research Journal, 20 (1) (2019) p. 6. https://doi.org/10.2478/aut-2019-0008

[21] M. Miao, Electrical conductivity of pure carbon nanotube yarns, Carbon, 49 (12) (2011), pp. 3755 – 3761.

[22] S. Chawla, M. Narahji, Effects of twist and porosity on the electrical conductivity of carbon nanofiber yarns, Nanotechnology, 24 (25) (2013) 255708. https://doi.org/10.1088/0957-24/25/255708

[23] F. Huang, H. Jiyong, X. Yan, Review of Fiber-on Yarn-Based Wearable Resistive Strain Sensors: Structural Design, Fabrication Technologies and Applications, Textiles, 2 (1) (2022), pp. 81 – 111. https://doi.org/10.3390/textiles2010005

[24] K. Keum, S.S. Cho, J. Jeong-Wan, S.K. Park, K. Yong-Hoon, Mechanically robust textile-based strain and pressure multimodal sensors using metal nanowire/polymer conducting fibers, iScience, 25 (4) (2022) 104032.

https://doi.org/10.1016/j.isci2022.104032

[25] S. Seyedin, P. Zhang, M. Naebe, S. Qin, J. Chen, X. Wang, J. M. Razal, Textile Strain Sensors: A Review of the Fabrication Technologies, performance Evaluation and Applications, Materials Horizons, 6 (2) (2019) pp. 219 – 249. https://doi.org/10.1039/C8MH01062E

[26] M. Ruppert-Stroescu, M. Balasubramanian, Effects of stitch classes on the electrical properties of conducive threads, Textile Research Journal, 88 (21) (2017), pp. 2454 – 2463. https://doi.org/10.1177/0040517517725116

[27] A. Vogl, P. Parzer, T. Babic, J. Leong, A. Olwal, M. Haller, StretchEBand: Enabling Fabric-based Interactions through Rapid Fabrication of Textile Stretch Sensors, in: CHI '17: Proceedings of the 2017 CHI Conference on Human Factors in Computing Systems, New York, (2017), pp. 2617 – 2627. https://doi.org/10.1145/3025453.3025938

[28] M. Martinez-Estrada, I. Gil, R. Fernández-García, Raúl, An Alternative Method to Develop Embroidery Textile Strain Sensors, Textiles, 1 (3) (2021), pp. 504 – 512. https://doi.org/10.3390/textiles1030026

[29] E. Dupler, L. Dunne, Effects of the Textile-Sensor Interface on Stitched Strain Sensor Performance In: ISWC'19: Proceedings of the 2019 ACM International Symposium on Wearable Computers, New York, (2019), pp. 45 – 53. https://doi.org/10.1145/3341163.3347717